Sasikumar, A., Trias, D., Costa, J., Blanco, N., Orr, J. i Linde, P. (2019). Impact and compression after impact response in thin laminates of spread-tow woven and non-crimp fabrics. *Composite Structures*, vol. 215, p. 432-445. Available online at
https://doi.org/10.1016/j.compstruct.2019.02.054

Impact and compression after impact response in thin laminates of spread-tow woven and non-crimp fabrics

A. Sasikumar[a,*], D. Trias[a,1], J. Costa[a,*], N. Blanco[a], J. Orr[b], P. Linde[c,d]

[a] *AMADE, Polytechnic School, University of Girona, Campus Montilivi s/n, 17073 Girona, Spain*
[b] *University of Dayton Research Institute, 300 College Park, Dayton, Ohio, USA*
[c] *Airbus Operations GmbH, Kreetslag 10, 21129 Hamburg, Germany*
[d] *Department of Industrial and Materials Science, Chalmers University of Technology, S-41296 Gothenburg, Sweden*

Abstract

Recent research has been devoted to thin laminates as a result of aeronautic industries shifting to thinner and lighter structures. In an attempt to improve the out-of-plane response and reduce manufacturing costs considerably, airplane manufacturers are exploring (apart from unidirectional tapes) textile fabrics of different fabric architectures. Within the framework of thin laminates, this paper investigates the impact and compression after impact (CAI) of two types of aerospace graded spread-tow fabrics, namely non-crimp fabrics and woven fabrics, where stitching and weaving, respectively, govern the architecture. The study also comprises two different ply thicknesses (thin and intermediate ply grades) for both fabrics. Experimental results reveal that while woven fabrics display higher damage resistance, non-crimp fabrics ensure higher damage tolerance. The intermediate ply grade performed better than thin plies in terms of damage resistance and CAI strength for both fabrics, as thin ply non-crimp fabric laminates exhibited early and extensive fibre damage.

Keywords: Non-crimp fabrics, Woven fabrics, Impact behaviour, Damage tolerance, Thin laminates

1. Introduction

In an attempt to go even lighter, aircraft industries are now considering how to reduce the thickness of many aircraft parts, such as wing and fuselage skins, to less than 2 mm. The threat posed by low velocity impact loads on these thin structures, accompanied by the change in the stress states and damage modes could be critical when compared to standard thick laminates [1; 2].

In the quest to improve the out-of-plane response, many concepts such as laminate design [3–5], interleaving [6], ply hybridization [2; 7], and the use of textile fabric composites have been explored [8]. Textile fabrics differ from uni-directional (UD) tapes in that the fibre tows are either woven, knitted, braided or stitched together in an attempt to enhance the mechanical performance and/or economic feasibility. Along with the efforts to reduce the structural weight of aircraft, the aeronautic industry

☆

*Corresponding author : Aravind Sasikumar, Josep Costa

Email addresses: aravind.sasikumar@udg.edu (A. Sasikumar), josep.costa@udg.edu (J. Costa)

[1] Serra Hunter Fellow

is also working on cutting back manufacturing costs and, as such, fabric composites have been an excellent substitute for UD tapes, thanks to their faster deposition rates and reduced labour time [9].

Out of the different reinforcement architectures, non-crimp fabrics (where UD layers are stitched) and woven fabrics (where UD tows are woven) have gained increasing attention in aerospace industries, mainly due to the improvement they offer over UD tapes in terms of higher interlaminar strength, better out-of-plane response and a considerable reduction in manufacturing costs [9; 10]. As textile composites have evolved, standard ply grade woven fabrics provided a substitute for UD prepreg tapes, with their main advantage being the increased toughness from the woven architecture and the reduced manufacturing costs related to the faster lay-up. Nevertheless, these same fabrics caused a reduction in in-plane properties as a result of their wavy fibres [11], thus non-crimp fabrics provided the solution. In non-crimp fabrics, the UD layers are stitched, therefore not only eliminating the problem of waviness, but also offering the economic feasibility of faster lay-up. Despite this, non-crimp fabrics exhibited local resin rich areas and fibre waviness around the stitch that impaired the compressive properties [12]. Another step forward was to employ thin plies (using spread tow technology) with woven fabrics which reduce considerably waviness and the magnitude of resin rich areas [13]. Despite the advances in textile composites, not many studies report on the effect the architecture of the fabric has on impact and post-impact responses, especially when used with thin laminates.

Vallons et al. [14] compared the interlaminar fracture toughness and impact damage resistance of carbon non-crimp fabrics and twill weave composite fabrics. The study employed different ply grade thicknesses (270 gsm for non-crimp fabrics and 190 gsm for woven) with (on average) 2.1 mm thick laminates. The woven fabrics exhibited higher fracture toughness and higher damage resistance compared to the non-crimp fabrics. Sanchez et al. [15] worked with thin laminates and compared the compression after impact (CAI) strength of woven fabrics with that of quasi-isotropic UD plies (both made out of thick plies) for laminate thicknesses ranging between 1.6 to 2.2 mm. Results evidenced that, compared to UD tapes, woven fabrics have a higher CAI strength, resulting from the increased interlaminar fracture toughness of woven fabrics. It is worth noting that both of these studies used non-standard specimen dimensions.

In the case of out-of-plane loading, thin plies have exhibited higher damage resistance and CAI strength, when used with thick laminates [16; 17]. Arteiro et al. [13] conducted an extensive experimental campaign to study the effect of spread tow fabric thickness on various structural properties. Thin woven fabrics, when compared with thick woven fabrics, exhibited a higher unnotched compression strength, an improved in-plane shear response and exhibited higher compressive resistance in off-axis compression tests. Similarly [18–20] with non-crimp fabrics, studies demonstrated the higher damage capability thin fabric plies have over thick ones in terms of structural performance. Meanwhile, Garcia et al. [21] studied the effect fabric thickness has on impact and CAI strength using non-crimp fabrics and demonstrating the sequence of failure events. Thin and standard ply grades were used with 2.15 mm laminates, and thin plies were reported to exhibit lower load carrying capability and lower CAI strength for a 14 J maximum impact energy level.

This paper is the result of a research project led by Airbus, in collaboration with the research centres INEGI (University of Porto, Portugal), UDRI (University of Dayton Research Institute, USA) and AMADE (University of Girona, Spain). We performed an experimental campaign on thin laminates using two types of aerospace grade fabrics, namely woven fabrics and non-crimp fabrics. In order to determine only the effect of the reinforcement architecture, both fabrics used in the study were made using the same fibre-resin material system. Additionally, for each fabric type we considered two different ply grades: thin and intermediate. Hence, this study reports the effects fabric architecture and ply thickness have on the impact and CAI response of thin composite laminates. The experimental campaign included impact and CAI tests to evaluate damage resistance and tolerance. Quasi-static indentation tests followed by C-scan damage inspection were also performed to study and compare the sequence of damage events.

2. Experimental methods

2.1. Material, fabric architecture and laminates

Two types of fabrics, namely spread-tow woven fabrics (WF) and spread-tow non-crimp fabrics (NCF), were processed at the University of Dayton Research Institute (UDRI) using carbon fibre T700 pre-impregnated with HexPly® M21 resin. Note that, to provide a proper comparison between the two types of fabrics, both fabrics were made using the same fibre-resin material system. WF are produced using a plain weave textile process where the weft fibre tows go over and under the warp tows, resulting in an interlaced woven fabric. Plain weave represents the weaving pattern where the weft tows cross over the warp tows continuously. While WF use weaving as the form of fabric architecture, NCF utilize a secondary stitching yarn that holds the fibre tows of different orientations together, forming a blanket. A bi-angle NCF is used in this study where two differently oriented fibre tows are stacked together like UD plies, and stitched together using a polyester yarn. Note that the sole purpose of the stitch is to permit a faster layup and is not intended to take structural loads.

Fig. 1 presents a schematic projected representation of both types of fabrics and also the macro photos of the fabric laminates used in this study. We used NCF bi-axial layers of [0°/45°] and [0°/-45°] whereas the WF comes in [0°/90°] fabric layers. Other fabric layer orientations can be obtained through rotation and flipping. Note that the mismatch angle within the fabric layer is 45° and 90° for NCF and WF, respectively.

[Figure 1 about here.]

In regards to the ply thickness study, two different areal weights per fabric layer were used. For NCF these were 268 gsm and 134 gsm and for WF 240 gsm and 160 gsm. As both fabrics are bi-axial, the ply thickness corresponds to half of the fabric tow thickness, namely 0.134 and 0.067 mm for NCF and 0.12 mm and 0.08 mm for WF, accounting for the intermediate and thin ply grades, respectively. From here on, the four laminates used throughout the study will be referred to as NCF-Int, NCF-Thin, WF-Int and WF-Thin. The laminates and their stacking sequences are illustrated in Fig. 2, while Table 1 details the laminates, their stacking sequences, ply and laminate thicknesses. All four laminates are not quasi-isotropic, and NCF-Int utilises non-conventional [22.5°/-22.5°] NCF fabric blankets obtained by rotating the standard blanket layer. Since the study utilizes different fabric materials and different ply thicknesses, the approach followed to obtain similar in-plane and flexural responses in the different laminates consists on pursuing the closest equivalent bending stiffness parameter (D*, proposed by Olsson [22], which is a function of the bending stiffness matrix coefficients) as possible. The D* values of NCF-Int, NCF-Thin, WF-Int and WF-Thin are 18.6, 18.9, 21.5 and 25.9 respectively. (Note that the nominal laminate thickness of woven fabrics is higher than the non-crimp fabrics which resulted in the higher D* values for the woven fabrics.) Figs. 3(a) and (b) present the polar plot of the in-plane and bending stiffness, respectively, for all four laminates.

[Figure 2 about here.]

[Table 1 about here.]

[Figure 3 about here.]

2.2. Impact energy definition

While both NCF laminates have the same laminate thicknesses, WF-Thin laminates displayed a higher measured laminate thickness compared to WF-Int (1.82 mm over 1.66 mm). However, when impacted at the same absolute impact energy, this might lead to misleading conclusions as a thicker laminate has an advantage over a thinner laminate. To avoid this bias, we defined two absolute and two normalized impact energies, where the normalization was performed with respect to the laminate thickness (as also suggested in ASTM D7136/D7136M-15 standards [23]). The authors are aware that this normalization will not guarantee 100% fair comparison, but still provides a fairer comparison. In total, four impact energies were explored, two absolute energies: 5 J and 10.5 J (referred to as IE_1 and IE_4, respectively) and two normalized energies: 4.1 J/mm and 5.2 J/mm (referred to as IE_2 and IE_3, respectively). Table 2 details the measured laminate thicknesses and the defined absolute and normalized impact energies for all laminates.

[Table 2 about here.]

2.3. Experimental tests

2.3.1. Impact, quasi-static indentation and damage assessment

In accordance with the ASTM D7136/D7136M-15 standards [23], impact tests were performed on 150 x 100 mm specimens using a CEAST Fractovis Plus instrumented drop-weight tower. The specimens were cut with the 0° fibres aligned with the specimen length. A 16 mm in diameter steel hemispherical indenter was used, and the total mass of the impactor setup was 3 kg. We impacted 12 specimens per laminate, with three specimens for each impact energy in order to assess repeatability. Further details of the experimental impact setup can be found in [24].

Quasi-static indentation (QSI) tests were performed with an MTS INSIGHT® 50 testing machine with a 50 kN load cell and displacement controlled loading of the indenter. The test setup replicates the impact test, where rubber clamps are placed at the four edges supporting the specimen. A 150 x 100 mm specimen was placed on a base plate, with an open window of 125 x 75 mm. A constant indenter displacement rate of 1 mm/min was used throughout the study. When a load drop or acoustic sound emission was noticed, tests were interrupted for C-scan damage inspection, followed by further indentation on the same specimen.

The main objective of QSI tests is to understand the onset and progression of the damage. As NCF-Int and NCF-Thin laminates have the same measured laminate thicknesses, they were tested under the same indenter displacement levels: d=3, 3.5, 3.95, 4.4, 4.7, 4.9, 5.3 and 6 mm. Initially the displacement levels for NCF-Int were decided arbitrarily, and then the same values were used for NCF-Thin in order to compare the damage sequence. Meanwhile, because of the differences in laminate thicknesses of the WF laminates, different indenter displacement levels were used. While WF-Int was indented at displacements d=2, 2.5, 3, 4.1, 5.6, 6.4 and 7 mm, WF-Thin was indented at d=2.5, 3.1, 4.1, 4.6, 5.1, 5.9 and 6.25 mm. Pulse-echo ultrasonic C-scan was used to inspect the damage from the impact and QSI tests. All the impacted and indented specimens after each indenter loading were inspected. C-scan inspection featured an OLYMPUS OMNI MX system and the specimens were placed in a pool of water while an automated robotic arm scanned them with a 5 MHz piezoelectric probe.

2.3.2. Plain strength compression and compression after impact

Prior to compression after impact, plain compression strength of all the laminates was determined following the ASTM D6484/D6484M-14 standard [25]. Plain compression tests were performed on three 305 mm x 30 mm specimens for each laminate at the INEGI research facility at the University of Porto. The interested reader can refer to [26] for more detailed information of the test setup.

Further, CAI tests were performed using an MTS INSIGHT®300 machine with a 300 kN load cell, following ASTM D7317/D7137M-15 [27]. As thin laminates were reported to fail under structural global buckling rather than a compressive failure [28], we used a non-standard anti-buckling CAI device as proposed by Remacha et al. [29]. This fixture ensures a proper compressive failure at the specimen centre induced by the existing impact damage. All the above-mentioned tests, except plain strength compression, were performed at the AMADE research laboratory at the University of Girona, which is NADCAP certified for non-metallic materials testing.

3. Experimental Results

3.1. Impact response

Figs. 4, 5 and 6 present the force-time, force-deflection, and energy-time impact curves, respectively, for all the laminates. While three specimens for each laminate and for each impact energy level were tested, because of the good repeatability in the responses, only one specimen per laminate has been presented in the impact curves. As the impact energies increase, NCF laminates lost their load carrying capacity compared to WF laminates, as evidenced by the reduced peak load (Figs. 4 and 5). Both NCF laminates exhibited significant load drops at the peak loads, which was more pronounced in NCF-Thin, associated to fibre failure. Unlike the other three laminates, NCF-Thin displayed longer response times (Fig. 4) and larger laminate bending (Fig. 5). Both WF laminates exhibited similar impact responses, except that WF-Thin displayed slight load drops for higher impact energies compared to WF-Int, which are associated with the initiation of fibre failure. NCF-Int performed better than NCF-Thin in terms of the peak load. In view of these comparisons, it is important to keep in mind that the in-plane and bending responses of the laminates are not exactly the same, owing to the different stacking sequence designs. Of all the laminates, NCF-Thin and WF-Int exhibited the highest and lowest energy dissipation, respectively (see Fig 6). For all the impact energies, WF laminates dissipated much less energy compared to NCF laminates. For both types of fabrics, intermediate ply grades exhibited better damage resistance than thin plies (more pronounced for the NCF laminates), in terms of reduced energy dissipation and increased load carrying capability.

[Figure 4 about here.]

[Figure 5 about here.]

[Figure 6 about here.]

Fig 7 shows the projected impact damage profile of all the laminates for all the impact energies obtained from the C-scan inspection. For all the impact energies except IE_1, NCF-Int exhibited a reduced projected damage area compared to its thin ply counterpart NCF-Thin. Dominant delaminations were identified for NCF-Int at interface 6 (-22.5°/22.5°, oriented in the 22.5° direction) and at the last interface (int 10: 0°/45°, oriented in the 45° direction). Note that the interfaces are numbered from the impacted surface with the last interface denoting the interface closest to the non-impacted side, as shown in Fig 2. For NCF-Thin, a dominant delamination oriented in the 0° direction was identified at interface 10 (-45°/0°) just above the mid-plane. Additionally for higher impact energies, C-scan images of NCF-Thin exhibited permanent indentation, which was not observed in other laminates.

[Figure 7 about here.]

[Figure 8 about here.]

Both WF laminates exhibited a close-to-circular projected delamination profile, as also observed in [30; 31] for plain woven fabrics. They showed similar projected damage profiles and areas for the chosen impact energies. WF-Int showed a dominant delamination at interface 9 (-45°/45°) oriented in 45°, whereas WF-Thin exhibited delaminations at various interfaces, making it difficult to pinpoint the dominant ones. Comparatively, WF displayed a much smaller damage area than NCF, and furthermore, while the delamination profile of NCF was controlled by one or two dominant delaminations, WF had several delaminated interfaces contributing to the overall contour.

Fig. 8 displays the photos of the impacted and non-impacted specimen faces from the 10.5 J impact (IE_4). NCF-Thin showed higher permanent dent depth and extensive back fibre splitting compared to intermediate ply grade NCF-Int. By contrast, the WF laminates displayed very little or negligible visible damage as compared to NCF laminates, neither was much visual difference in dent depth and back face splitting observed between the WF laminates.

[Figure 9 about here.]

[Figure 10 about here.]

Figs. 9 (a) and (b) present the evolution of the peak load and projected damage area, respectively, for the increasing absolute impact energies of all the laminates. When compared with NCF-Int, NCF-Thin showed a reduced load carrying capacity, a 13% reduction in peak load for IE_1 and IE_2 and 27% for IE_3 and IE_4. Similarly, NCF-Thin exhibited a 30% increase in the projected impact damage area over NCF-Int for the higher impact energies. WF-Int and WF-Thin roughly exhibited the same peak load and projected damage area, showing the negligible effect that ply thickness has on these damage resistance parameters. Within the two fabric types, WF displayed higher damage resistance over NCF, evidenced by the higher peak load for all impact energies and reduced damage area, especially at the higher impact energies.

Figs. 10 (a) and (b) display the dissipated energy and the impact dent depth, respectively, for all the absolute impact energies. At lower impact energies, both NCF laminates exhibited roughly the same dent depth, whereas for higher energies NCF-thin showed twice the dent depth compared to NCF-Int (as can also be seen in Fig. 8). The WF laminates displayed similar dent depth values, and when NCF and WF were compared, woven fabrics clearly exhibited lower dent depth. Both thin-ply fabrics (NCF-Thin and WF-Thin) showed higher energy dissipation compared to their intermediate-ply counterparts. As observed for other parameters, WF laminates exhibit better damage resistance by dissipating less energy than NCF laminates do.

3.2. Quasi-static indentation

Fig. 11 compares the force-deflection response of the maximum applied indenter displacement (d_8= 6 mm) of both NCF laminates. The other displacement levels studied, along with the respective energies applied (E_a), are also marked on the same figure. As observed with the impact results, QSI tests also showed reduced peak load and intermittent load drops with NCF-Thin, where the first visible load drop was observed at d_3= 4 mm, when compared to the delayed first load drop at d_7= 5.5 mm with NCF-Int. The projected damage contours obtained from the interrupted C-scan damage inspection for all the indenter displacement levels of NCF laminates are compared in Fig. 12.

[Figure 11 about here.]

[Figure 12 about here.]

NCF-Thin exhibited delayed damage onset over NCF-Int (as in Fig. 12), where displacement d_1 results exhibited the initiation of delamination damage in NCF-Int (evidenced below the mid-plane at interface 7: -22.5°/22.5°), but there was no presence of damage in NCF-Thin. Displacement level d_2 provided an increase in the delamination area for NCF-Int, with new delaminated interfaces at the top (interface 5: 22.5°/-22.5°), meanwhile displacement d_3 marked the onset of delamination damage in NCF-Thin at the last interface (0°/45°). Mild intermittent cracking sounds were heard from NCF-Int in the loading stages starting from d_1, whereas the first acoustic emission for NCF-Thin was noticed at d_3, and was associated with the fibre splitting observed on the back face of the laminate and the first load drop. From displacements d_4 to d_6, the delamination profile scaled up with NCF-Int, and a dominant delamination oriented in the 0° direction, just above the mid-plane (interface 11; -45°/0°), was observed for NCF-Thin. Displacement d_7 resulted in the back fibre splitting of NCF-Int, evidenced by a load drop, whereas NCF-Thin underwent further fibre failure which induced a higher delamination area when compared to NCF-Int.

Moving on to woven fabrics, Figs. 13 (a) and (b) present the force-deflection response of WF-Int and WF-Thin, respectively, for their maximum applied indenter displacement ($d = 7$ mm for WF-Int and

$d = 6.25$ mm for WF-Thin). Note that, unlike the NCF laminates, the WF laminates were indented at different displacement levels, due to their different laminate thicknesses, and hence the sole aim is to study the damage evolution rather than make comparisons. Fig. 13 also presents the other indenter displacements studied and their corresponding applied energies. C-scan inspection images of both WF laminates are presented in Fig. 14 aligned along the different deflection levels in the horizontal axis.

WF-Int displayed no load drop in the force response curve during the loading stages, and the first load drop was seen at the maximum load (between d_6 and d_7). In Fig. 14, no damage was observed for the d_1 displacement, whereas damage initiation was noticed at d_2 in the C-scan images. Delamination initiation was identified at interfaces 5 (45°/-45°), 9 (-45°/45°), 13 (-45°/45°) and all these interfaces correspond to interfaces within the fabric blanket. This could possibly be due to the higher mismatch angle within the fabric blanket. Despite no sign of load drop in the force-displacement curve, C-scan inspection showed that sufficient damage was formed in the laminate. With continued loading, the delamination contour enlarged and new delaminated interfaces appeared. We observed traces of back fibre splitting between displacements d_6 and d_7. The higher capability of standard ply grade woven fabrics to delay or suppress fibre failure is illustrated here, as the first sign of failure was observed at an applied energy, E_a, of 14 J.

In the case of WF-Thin, the first load drop was observed before the maximum load (between d_5 and d_6), and a further larger drop at the maximum peak load. As with NCF-Thin, back fibre splitting was observed at the point of the first load drop. The first sign of delamination (Fig. 14) was observed at displacement d_2, where interfaces 12 (45°/-45°) and 14 (45°/90°), both below the mid-plane, were found to be delaminated. Even though it is not open for direct comparison, it can be seen that WF-Thin delayed the onset of damage and accelerated the onset of fibre failure; something also observed with NCF-Thin. With further loading, new interfaces amounted to the existing delaminations, and the projected damage contours were roughly the same as for WF-Int. Additionally, a good coherence was seen between the results of the impact and QSI tests in terms of projected delamination profile, area and the force level of fibre failure initiation for both types of fabrics.

[Figure 13 about here.]

[Figure 14 about here.]

3.3. Plain compression and compression after impact

Figs. 15 (a) and (b) present both pristine compression and compression after impact strength values for all laminates for absolute and normalized impact energies, respectively. The thin plies displayed a better plain compression strength than the intermediate plies: NCF-Thin and WF-Thin displayed 10% and 7% increase over their intermediate grade counterparts. An average increase of 15% in plain compression strength was observed for non-crimp fabrics when compared to woven fabrics (as in Fig 15).

[Figure 15 about here.]

Despite the use of an anti-buckling device, improper CAI failure at the specimen top (local buckling at the open top window of the fixture, instead of being at the impacted zone) was observed for laminates impacted at lower impact energies (as also reported in [2; 28] for thin laminates). All the laminates impacted at IE_1 and all the laminates impacted at IE_2, except NCF-Int, exhibited CAI failure at the top of the specimen due to local buckling. The laminates and the CAI values corresponding to improper CAI failure are also indicated in Fig. 15.

Plain compression and CAI strength values of all the laminates normalized with respect to NCF-Thin and WF-Thin values are presented in Figs. 16 (a) and (b), respectively. Intermediate grade plies showed higher CAI strength than thinner plies did and this was more pronounced for the NCF laminates. NCF-Int showed on average a 20% higher CAI strength than NCF-Thin (see IE_3 and IE_4 in Fig. 16 (a)), while WF-Int exhibited slightly higher CAI strength (9% for IE_3) over WF-Thin (Fig. 16 (b)).

[Figure 16 about here.]

In a more detailed overview from all of the laminates, NCF-Int exhibited improved CAI strength (considering valid CAI values from IE_3 and IE_4 energies). Reviewing IE_3, NCF-Int displayed 20% higher CAI strength than NCF-Thin and WF-Int, and close to 30% higher than WF-Thin. Moving to IE_4, both WF-Int and WF-Thin showed better CAI strength than NCF-Thin, by 10% and 7%, respectively, whereas NCF-Int showed 16% higher CAI strength over its thin ply NCF. In terms of strength retention, NCF-Thin displayed the highest reduction (65%) in residual compression strength induced by the extensive fibre damage from impact (Fig. 17), whereas the WF laminates exhibited a reduction of approximately 50% in compression strength.

[Figure 17 about here.]

4. Discussion

4.1. Impact damage resistance

As evidenced by the experimental results, the woven fabrics exhibited better impact damage resistance than non-crimp fabrics did. The significant load drops reported for the NCF laminates are related to the initiation of fibre failure (see Fig. 5), as was also evidenced in the QSI results. At the same time, the absence of such load drops in the WF laminates suggests the reduced and delayed presence of fibre failure. The significant increase of the impact damage related parameters (Figs. 9 and 10) for NCF over WF also supports the escalation of fibre breakage in NCF at higher impact energy levels. It is important to keep in mind that the thin ply of NCF (67 gsm) is thinner than its WF counterpart (80 gsm), so the effect of the reduced ply thickness is more pronounced.

The higher damage resistance of woven fabrics is associated with their increased interlaminar fracture toughness. As a result of the woven architecture, the fibre tows have undulations/waviness and both the weft and warp tows are present in the same interface. Therefore, as a crack propagates at an interface, it follows a wavy path due to the waviness of the fibre tows, and further, as the crack encounters a different oriented fibre tow, the crack front jumps to follow this direction. All this results in an increased effective crack length and an excess energy dissipation, thereby an increased fracture toughness [10; 14]. On the other hand, NCF fibre tows are rather straight like UD tapes, except for the fact that two UD plies are stitched together. They are reported to have a reduced interlaminar fracture toughness compared to woven fabrics [14], thereby demonstrating the effect of woven reinforcement architecture.

WF laminates exhibited more delaminated interfaces and a reduced projected area compared to NCF. QSI results revealed that most delaminations were formed within the WF fabric blanket, which can be due to the higher mismatch angle of 90° within the fabrics that favours delamination [3]. The reduced projected damage area of WF is reasoned to be either the higher number of delaminated interfaces or the delamination propagation being suppressed by the increased mode II fracture toughness of the woven fabrics, where the delamination cannot extend easily as it is forced to change its plane following the weft and warp. Further, the magnitude of fibre failure is far smaller in WF laminates compared to NCF. The delamination onset for WF laminates happens before delamination onset for NCF laminates (as in Figs. 12 and 14), and this could probably delay the fibre damage onset. In addition, the interwoven fabric architecture may help to suppress the escalation of fibre damage. When a fibre bundle of a weft tow fails, the warp tows may help to re-distribute the stresses. Micro X-ray tomography investigations could help to obtain a proper understanding and can be employed in future work.

In analysing the ply thickness effect, thin laminates, due to the reduced bending stiffness, underwent significant bending during impact loads which led to high tensile stresses at the non-impacted laminate face. Because of the inherent in-situ effect of thin plies and lower interlaminar stresses, NCF-Thin delayed the onset of matrix cracking and consequently delaminations. However, with the delayed damage onset, early fibre failure was evidenced in NCF-Thin, as seen through the significant load drops in the impact response curves and also the early fibre splitting at the laminate back face evidenced in QSI results (Fig. 11 and Fig. 12). Even though delamination onset was suppressed, extensive delamination was observed after fibre failure in thin ply laminates (as reported in [32]), thus NCF-thin exhibited a higher projected damage area over NCF-Int at higher energies. On the other hand, early matrix cracking and delaminations in NCF-Int delayed and reduced the intensity of fibre failure by having less energy available for the fibre damage process.

The same explanation is valid for the greater damage resistance of WF-Int over WF-Thin, even though the improvement is marginal when compared with the NCF laminates. The roughly similar damage resistance response of the WF laminates may be due to the ply grades chosen for the study, as the difference between the thin ply grade (80 gsm) and standard ply grade (120 gsm) was not as significant as in the case of NCF laminates (67 vs 134 gsm). Delamination initiation and its location were evidenced in the QSI results, which otherwise would not have been able to be detected from the impact results. NCF-Int exhibited delaminations above and below the mid-plane cluster ply formed due to symmetry axis, and this cluster introduces high bending stiffness mismatch between the adjacent interfaces, leading to high interlaminar shear stresses. The same can be seen with NCF-Thin just below the mid-plane.

4.2. Impact damage tolerance

An average 15% lower plain compression strength was observed on woven fabrics when compared to non-crimp fabrics. With the same fibre-resin material system for both types of fabrics, the reduction in the in-plane compressive strength is related to the fibre tow waviness of the woven fabrics [11]. It should also be kept in mind that the ply ratio along each orientation is not the same for NCF and WF laminates. Despite this, the waviness is greatly reduced in spread-tow woven fabrics compared to conventional ones [13; 33; 34]. The minimal waviness causes the in-plane properties of woven fabrics to be extremely close to that of the UD tapes. However, the minimal but inevitable waviness induces fibre kinking under compressive loading that impairs the compressive strength. Therefore, the same woven fibre architecture which helped to increase the damage resistance and fracture toughness, counteracted this with reduced CAI strength.

On the ply thickness effect, thin plies demonstrated an increased plain compression strength (10% for NCF and 7% for WF) over their intermediate ply counterparts. Thin plies possess increased longitudinal compression strength mainly attributed to the uniform micro-structure of the thin spread-tow, less waviness associated with thin plies, thus leading to fewer resin rich areas [13; 35]. In the framework of compression after impact, as discussed in the previous section, the behaviour thin plies possess characterised by early and extensive fibre failure (because of delayed matrix cracks and delamination) has resulted in the reduced CAI strength thin ply laminates demonstrate (also reported in [2]). Contrary to the thick or standard laminates, where thin plies improved the CAI strength over thicker plies [16], thin plies used with thin laminates have led to increased fibre failure leading to reduced CAI strength. As explained earlier, thin plies dissipated most of their energy through fibre failure, whereas the intermediate plies do this through delamination. The final collapse of the specimen during CAI loading is mainly driven by the impact induced fibre damage than by the delamination, as is seen in the case of thin laminates.

4.3. Thin laminates and masked delamination load drops

Contrary to the thick or standard laminates, the thin laminates exhibited no signs of load drop in the initial stages of loading, where the initiation and propagation of delaminations are literally hidden in the force response curves. This is clearly seen from the QSI results for both NCF and WF laminates, where a delamination observed in the C-scan inspection is not represented by any load drop in the force response curve. As reported in [36], this is explained as an effect of the reduced laminate thickness. The force-deflection response curve of a laminate is the sum of the bending and membrane-stretching stiffnesses of the laminate. At higher deflections, where the membrane-stretching is dominant, the delaminations and their associated load drop have little influence on membrane behaviour. Hence, the significant load drops encountered in the force responses of the thin laminates is related to fibre damage, where the in-plane membrane stiffness drops due to the damaged fibres. Therefore, unlike the thick laminates, the force responses of the thin laminates does not signal the initiation or development of matrix and delamination damage through load drops, as these are only detected through damage inspections.

4.4. Damage tolerance in terms of damage detectability

One of the ultimate goals of the research community is to improve the damage tolerance of a structure. That is, the ability of the structure to have enough residual strength to carry post-impact service loads until the impact damage has been detected. It is also equally important for impact damage to be detected during service inspections so that it can be repaired and a final structural collapse avoided [37; 38]. Impact damage is normally detected through the permanent impact dent depth formed on the impacted surface. It has been reported that a dent depth between 0.25 to 0.5 mm deep is highly likely to be detected [39]. When comparing NCF and WF laminates in this framework, WF laminates exhibited less than 0.1 mm dent depth even at the highest impact energy, while NCF showed three or four times higher dent depth, thereby increasing their chances of being detected (as in Fig. 8). Moreover,WF laminates displayed a reduced residual strength which leads to a worse scenario as the damage can be left undetected, and at the same time they do not have a higher residual strength to withstand the loads. NCF outperform WF laminates in this, because the chances of detecting the damage is greater and also they have higher residual strength.

In a recent work by the authors [2], we carried out a similar study with UD tapes (using the same fibre-resin material as in this paper) considering different ply thicknesses. Comparing the impact and post-impact performance of fabrics with UD tapes (note that the UD baseline considered here is the intermediate ply grade of 134 gsm), the damage resistance of UD tapes and non-crimp fabrics is very similar, whereas the woven fabrics exhibit a superior performance compared to both UD and NCF. Meanwhile, non-crimp fabrics, NCF-Int exhibit considerably higher impact tolerance values (about 15%) than UD and there were similar CAI values between the UD and the woven fabric WF-Int.

4.5. Textile fabrics: prospects and further work

The study concludes that woven fabrics have good damage resistance, while NCF have a higher residual strength for post-impact loads and also favour impact damage detectability. Hence, these fabrics can be customized according to particular aircraft structures and the type of loads encountered. As a further improvement, laminates can be designed with hybrid designs at the ply level, where the standard and the thin ply grades can be mixed in the same laminate, as was done by the authors with UD plies [2]. The standard plies help to reduce the magnitude of fibre failure by dissipating energy through delaminations, while the thin plies and their improved compressive strength help in post-impact compressive loads. For woven fabrics, the means of improvement is to have the least reduction in the in-plane compressive properties when compared to UD plies, which is a key factor in improving post-impact residual strength. Since the woven fabric architecture helps to improve the fracture toughness and at the same time reduces the in-plane compressive properties, a balance between these two features should be made. One of the options is to substitute $0°$ fabric layers with UD $0°$ plies, where the undistorted $0°$ plies provide the residual strength during the in-plane compressive loading of CAI [40].

5. Conclusion

We carried out an experimental campaign to study the effect of fabric reinforcement architecture and tow thickness on the impact and compression after impact response of thin laminates (1.6 - 1.8 mm). We used two types of aerospace graded fabrics, namely non-crimp fabrics and woven fabrics, where two UD layers/tows were stitched and weaved together, respectively. In addition, two different tow thicknesses (standard and thin ply grade) were used for each fabric. Impact results revealed that woven fabrics undoubtedly exhibited a superior impact damage resistance, evidenced by the 50% less dissipated energy, reduced dent depth and projected damage area over the non-crimp fabrics. In terms of ply thickness effect, thin plies with thin laminates delayed the onset of cracks and delamination, but displayed early fibre failure, especially with non-crimp fabrics. This was demonstrated through quasi-static indentation tests, where the entire sequence of damage evolution was compared. The intermediate ply grade exhibited improved damage resistance (50% and 45% less energy dissipated for NCF and WF, respectively) over thin plies. Despite a lower impact damage resistance, non-crimp fabrics displayed an average 20% higher CAI strength over the woven fabrics. In addition, intermediate ply grade exhibited higher post-impact residual strength (20% and 10% higher CAI strength for NCF and WF, respectively) over their thin ply counterparts. With textile fabrics being a good economic prospect, future work can be dedicated to mixing plies of different thicknesses in the same laminate, thereby aiming to improve the damage tolerance.

Acknowledgements

The first author would like to thank the Generalitat de Catalunya for the FI-DGR pre-doctoral grant 2018 FI-B2 00118. Josep Costa would like to thank the *Spanish Ministerio de Economía y Competitividad* for the grant coded MAT2015-69491-C3-1-R supported by FEDER/EU. The study is part of an extensive project funded by Airbus, partnered by the AMADE research laboratory (University of Girona), INEGI research group (University of Porto), and the University of Dayton Research Group. The authors would like to thank the University of Dayton Research Institute (UDRI) for manufacturing the specimens. Thanks also go to Prof. Pedro P. Camanho and the colleagues from the INEGI group for performing and sharing the plain compression strength results.

Data Availability

The raw/processed data required to reproduce these findings cannot be shared at this time due to legal or ethical reasons.

References

[1] S. Abrate, Impact on Composite Structures, Cambridge University Press, 2005.

[2] A. Sasikumar, D. Trias, J. Costa, N. Blanco, J. Orr, P. Linde, Effect of ply thickness and ply level hybridization on compression after impact strength of thin laminates, Submitted to Composites Part A: Applied Science and Manufacturing.

[3] T. Sebaey, E. González, C. Lopes, N. Blanco, P. Maimí, J. Costa, Damage resistance and damage tolerance of dispersed CFRP laminates: Effect of the mismatch angle between plies, Composite Structures 101 (2013) 255–264.

[4] Y. Liv, G. Guillamet, J. Costa, E. González, L. Marín, J. Mayugo, Experimental study into compression after impact strength of laminates with conventional and nonconventional ply orientations, Composites Part B: Engineering 126 (2017) 133–142.

[5] A. Sasikumar, J. Costa, D. Trias, E. V. González, S. García-Rodríguez, P. Maimí, Unsymmetrical stacking sequences as a novel approach to tailor damage resistance under out-of-plane impact loading, Composites Science and Technology 173 (2019) 125–135.

[6] S. García-Rodríguez, J. Costa, V. Singery, I. Boada, J. Mayugo, The effect interleaving has on thin-ply non-crimp fabric laminate impact response: X-ray tomography investigation, Composites Part A: Applied Science and Manufacturing 107 (2018) 409–420.

[7] T. Sebaey, E. Mahdi, Using thin-plies to improve the damage resistance and tolerance of aeronautical CFRP composites, Composites Part A: Applied Science and Manufacturing 86 (2016) 31–38.

[8] G. Bibo, P. Hogg, The role of reinforcement architecture on impact damage mechanisms and post-impact compression behaviour, Journal of Materials Science 31 (5) (1996) 1115–1137.

[9] G. Bibo, P. Hogg, R. Backhouse, A. Mills, Carbon-fibre non-crimp fabric laminates for cost-effective damage-tolerant structures, Composites Science and Technology 58 (1) (1998) 129–143.

[10] J.-K. Kim, M.-L. Sham, Impact and delamination failure of woven-fabric composites, Composites Science and Technology 60 (5) (2000) 745–761.

[11] Y. Mahadik, S. Hallett, Effect of fabric compaction and yarn waviness on 3D woven composite compressive properties, Composites Part A: Applied Science and Manufacturing 42 (11) (2011) 1592–1600.

[12] S. V. Lomov, Non-crimp fabric composites: manufacturing, properties and applications, Elsevier, 2011.

[13] A. Arteiro, G. Catalanotti, J. Xavier, P. Linde, P. Camanho, Effect of tow thickness on the structural response of aerospace-grade spread-tow fabrics, Composite Structures 179 (2017) 208–223.

[14] K. Vallons, A. Behaeghe, S. V. Lomov, I. Verpoest, Impact and post-impact properties of a carbon fibre non-crimp fabric and a twill weave composite, Composites Part A: Applied Science and Manufacturing 41 (8) (2010) 1019–1026.

[15] S. Sánchez-Sáez, E. Barbero, R. Zaera, C. Navarro, Compression after impact of thin composite laminates, Composites Science and Technology 65 (13) (2005) 1911–1919.

[16] S. Sihn, R. Y. Kim, K. Kawabe, S. W. Tsai, Experimental studies of thin-ply laminated composites, Composites Science and Technology 67 (6) (2007) 996–1008.

[17] T. Yokozeki, Y. Aoki, T. Ogasawara, Experimental characterization of strength and damage resistance properties of thin-ply carbon fiber/toughened epoxy laminates, Composite Structures 82 (3) (2008) 382–389.

[18] C. Furtado, A. Arteiro, G. Catalanotti, J. Xavier, P. Camanho, Selective ply-level hybridisation for improved notched response of composite laminates, Composite Structures 145 (2016) 1–14.

[19] A. Arteiro, G. Catalanotti, J. Xavier, P. Camanho, Large damage capability of non-crimp fabric thin-ply laminates, Composites Part A: Applied Science and Manufacturing 63 (2014) 110–122.

[20] A. Arteiro, G. Catalanotti, J. Xavier, P. Linde, P. Camanho, A strategy to improve the structural performance of non-crimp fabric thin-ply laminates, Composite Structures 188 (2018) 438–449.

[21] S. García-Rodríguez, J. Costa, A. Bardera, V. Singery, D. Trias, A 3D tomographic investigation to elucidate the low-velocity impact resistance, tolerance and damage sequence of thin non-crimp fabric laminates: effect of ply-thickness, Composites Part A: Applied Science and Manufacturing 113 (2018) 53–65.

[22] R. Olsson, Closed form prediction of peak load and delamination onset under small mass impact, Composite Structures 59 (3) (2003) 341–349.

[23] ASTM D7136/D7136-15, Standard test method for measuring the damage resistance of a fiber reinforced polymer matrix composite to a drop weight impact event, 2015.

[24] E. González, P. Maimí, P. Camanho, C. Lopes, N. Blanco, Effects of ply clustering in laminated composite plates under low-velocity impact loading, Composites Science and Technology 71 (6) (2011) 805–817.

[25] ASTM D6484/D6484M-09, Standard test method for open-hole compressive strength of polymer matrix composite laminates, 2009.

[26] A. Arteiro, G. Catalanotti, J. Xavier, P. Camanho, Notched response of non-crimp fabric thin-ply laminates, Composites Science and Technology 79 (2013) 97–114.

[27] ASTM D7137/D7137-15, Standard Test Method for Compressive Residual Strength Properties of Damaged Polymer Matrix Composite Plates, 2015.

[28] D. Ghelli, G. Minak, Low velocity impact and compression after impact tests on thin carbon/epoxy laminates, Composites Part B: Engineering 42 (7) (2011) 2067–2079.

[29] M. Remacha, S. Sánchez-Sáez, B. López-Romano, E. Barbero, A new device for determining the compression after impact strength in thin laminates, Composite Structures 127 (2015) 99–107.

[30] E. González, P. Maimí, E. Martín-Santos, A. Soto, P. Cruz, F. M. de la Escalera, J. S. de Aja, Simulating drop-weight impact and compression after impact tests on composite laminates using conventional shell finite elements, International Journal of Solids and Structures 144 (2018) 230–247.

[31] A. Soto, E. González, P. Maimí, F. M. de la Escalera, J. S. de Aja, E. Alvarez, Low velocity impact and compression after impact simulation of thin ply laminates, Composites Part A: Applied Science and Manufacturing 109 (2018) 413–427.

[32] H. Saito, M. Morita, K. Kawabe, M. Kanesaki, H. Takeuchi, M. Tanaka, I. Kimpara, Effect of ply-thickness on impact damage morphology in CFRP laminates, Journal of Reinforced Plastics and Composites 30 (13) (2011) 1097–1106.

[33] H. M. EL-Dessouky, C. A. Lawrence, Ultra-lightweight carbon fibre/thermoplastic composite material using spread tow technology, Composites Part B: Engineering 50 (2013) 91–97.

[34] M. Shamsudin, C. York, Mechanically coupled laminates with balanced plain weave, Composite Structures 107 (2014) 416–428.

[35] R. Amacher, J. Cugnoni, J. Botsis, L. Sorensen, W. Smith, C. Dransfeld, Thin ply composites: experimental characterization and modeling of size-effects, Composites Science and Technology 101 (2014) 121–132.

[36] J. Lee, C. Soutis, Prediction of impact-induced fibre damage in circular composite plates, Applied Composite Materials 12 (2) (2005) 109–131.

[37] C. Bouvet, S. Rivallant, J.-J. Barrau, Low velocity impact modeling in composite laminates capturing permanent indentation, Composites Science and Technology 72 (16) (2012) 1977–1988.

[38] S. Rivallant, C. Bouvet, N. Hongkarnjanakul, Failure analysis of cfrp laminates subjected to compression after impact: FE simulation using discrete interface elements, Composites Part A: Applied Science and Manufacturing 55 (2013) 83–93.

[39] N. Hongkarnjanakul, Modélisation numérique pour la tolérance aux dommages d'impact sur stratifié composite: de l'impact à la résistance résiduelle en compression, PhD thesis, ISAE, Toulouse.

[40] P. Curtis, S. M. Bishop, An assessment of the potential of woven carbon fibre-reinforced plastics for high performance applications, Composites 15 (4) (1984) 259–265.

List of Figures

List of Tables

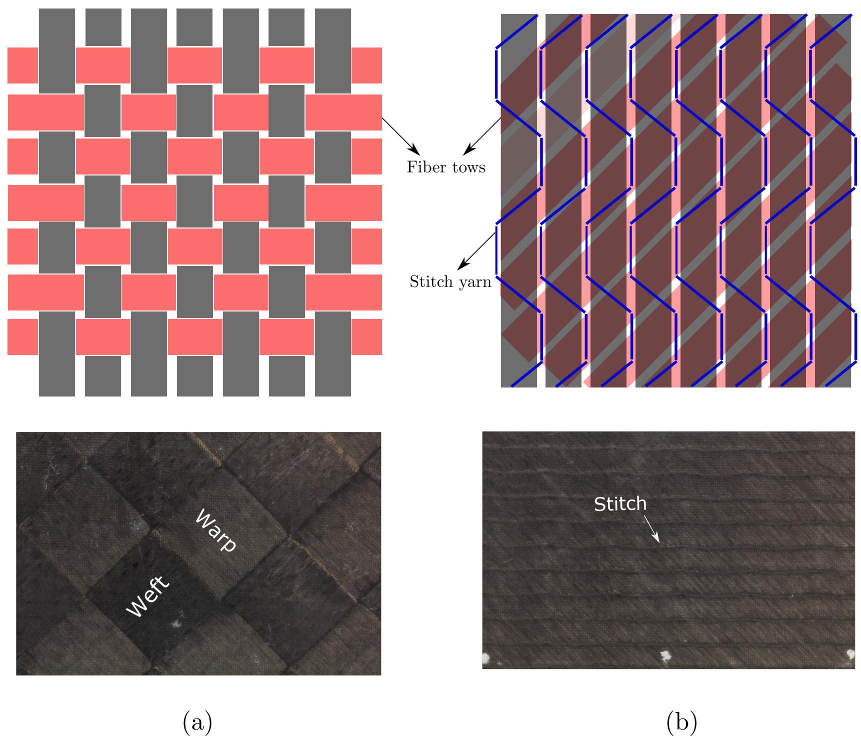

Figure 1: 2D planar illustration of the fabrics and their architecture (a) Woven fabrics (WF) with plain weave (b) Non-crimp fabrics (NCF) with plies stitched together using a polyester yarn.

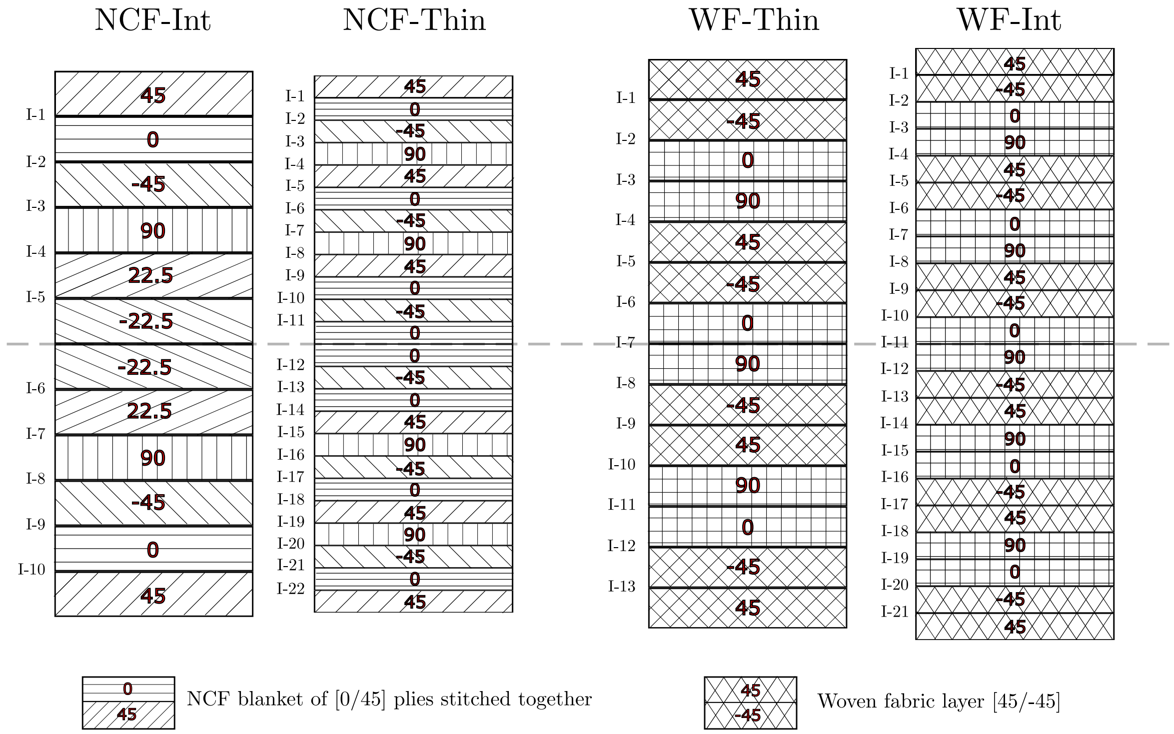

Figure 2: Schematic illustration of the laminates and their stacking sequences: Non-crimp fabrics (NCF) and Woven fabrics (WF).

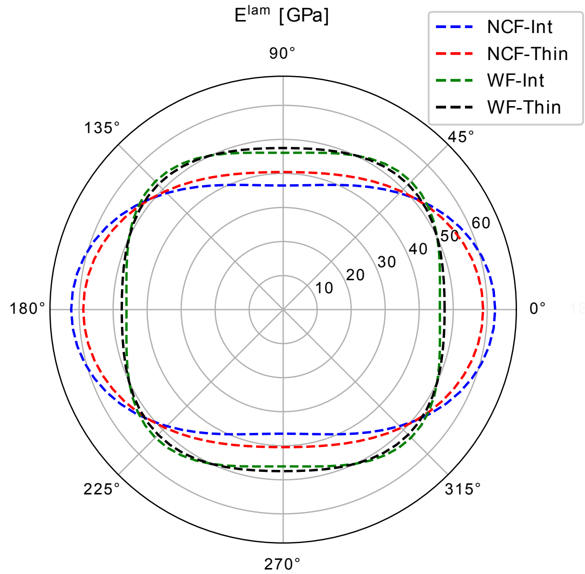

(a)

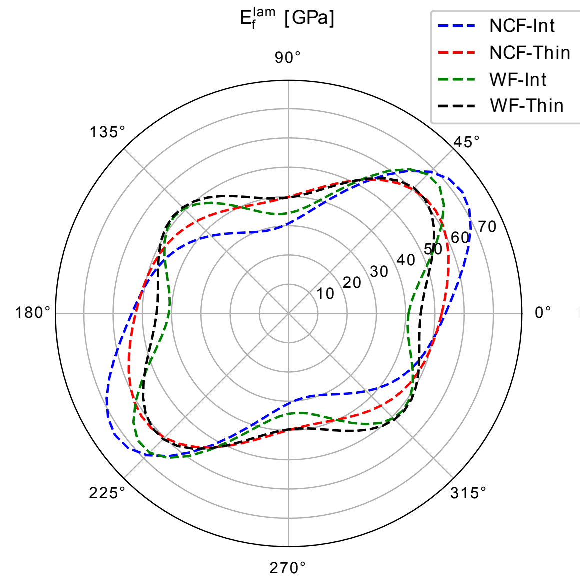

(b)

Figure 3: Polar plot representation of the (a) in-plane stiffness and (b) bending stiffness for all the laminates.

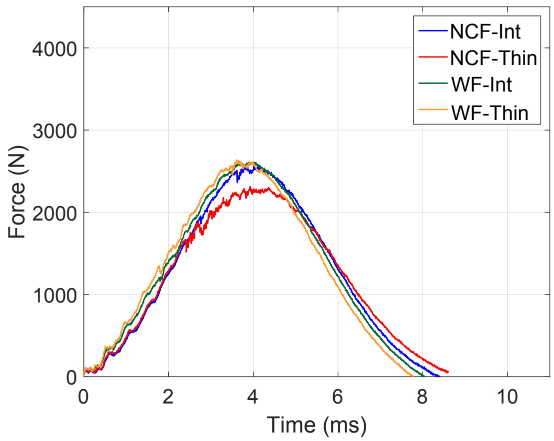

(a) IE_1

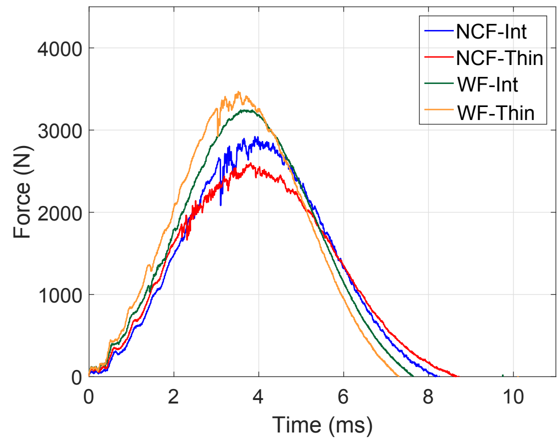

(b) IE_2

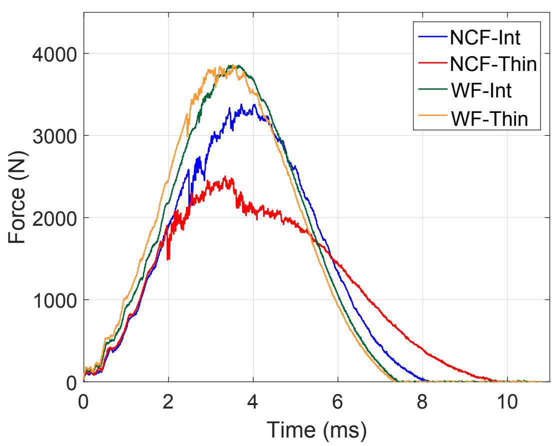

(c) IE_3

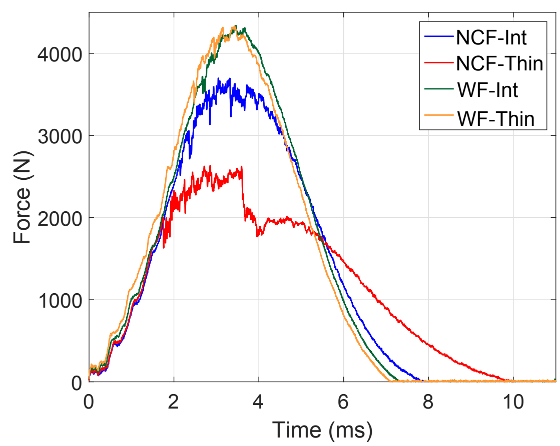

(d) IE_4

Figure 4: Force-time responses of all the laminates for all the impact energies.

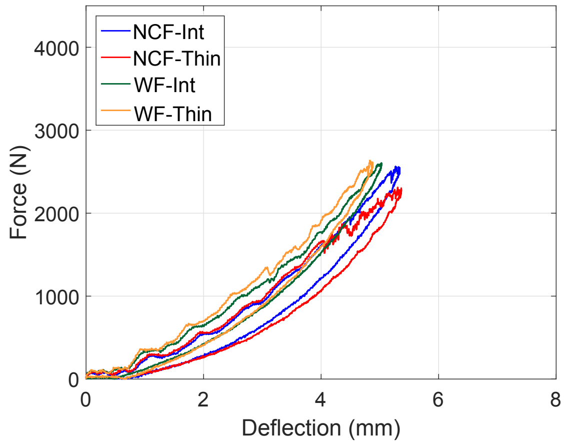

(a) IE_1

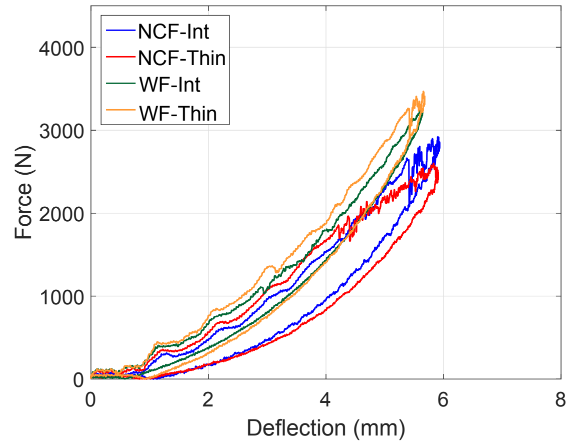

(b) IE_2

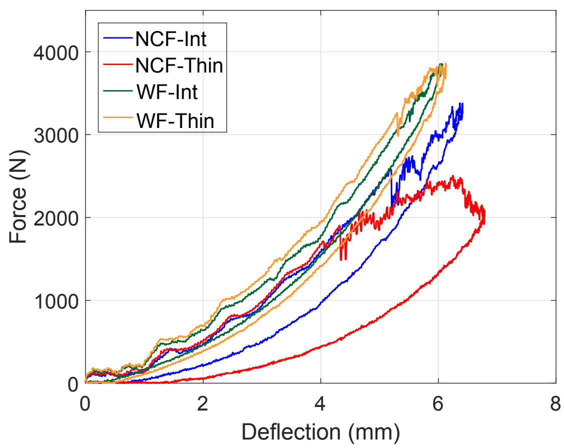

(c) IE_3

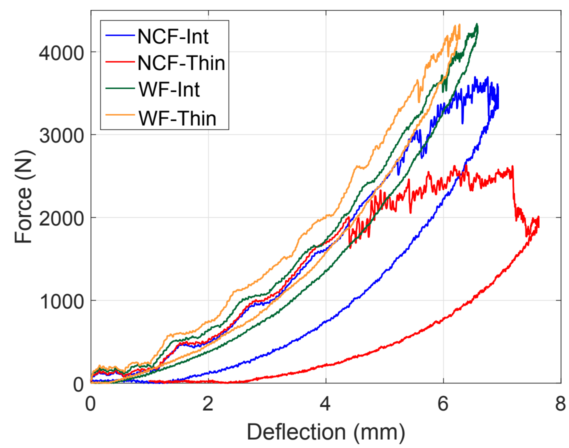

(d) IE_4

Figure 5: Force-displacement responses of all the laminates for all the impact energies.

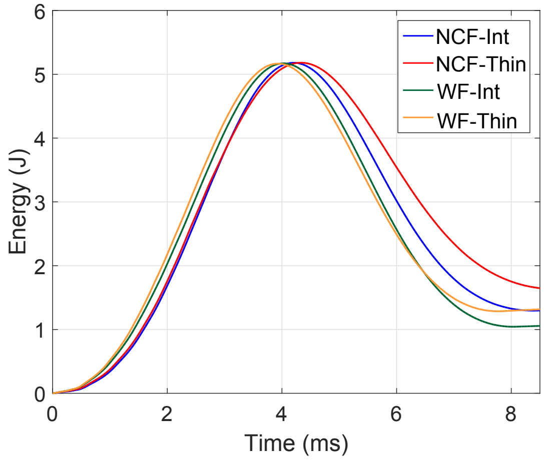

(a) IE_1

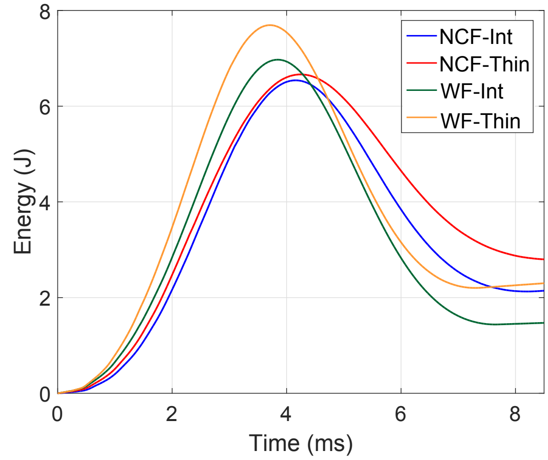

(b) IE_2

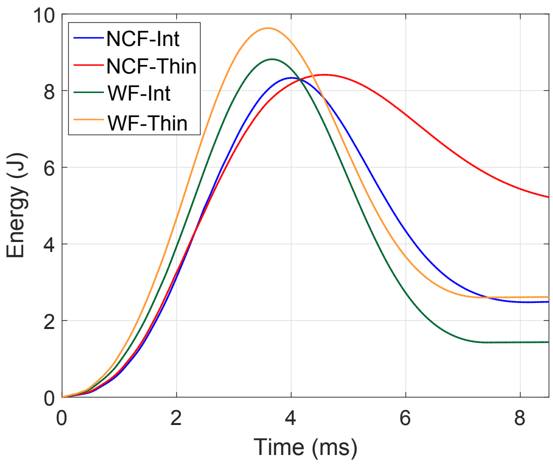

(c) IE_3

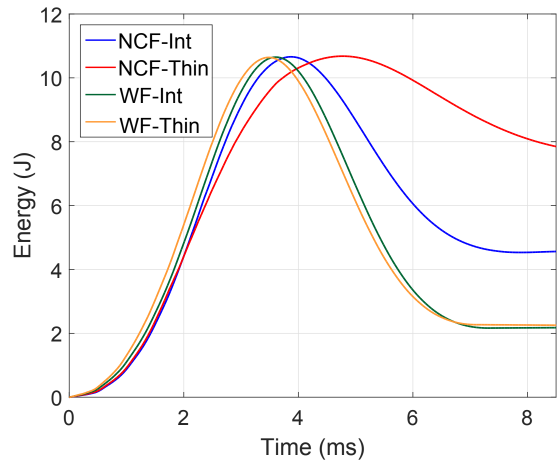

(d) IE_4

Figure 6: Impact energy evolution of all the laminates for all the impact energies.

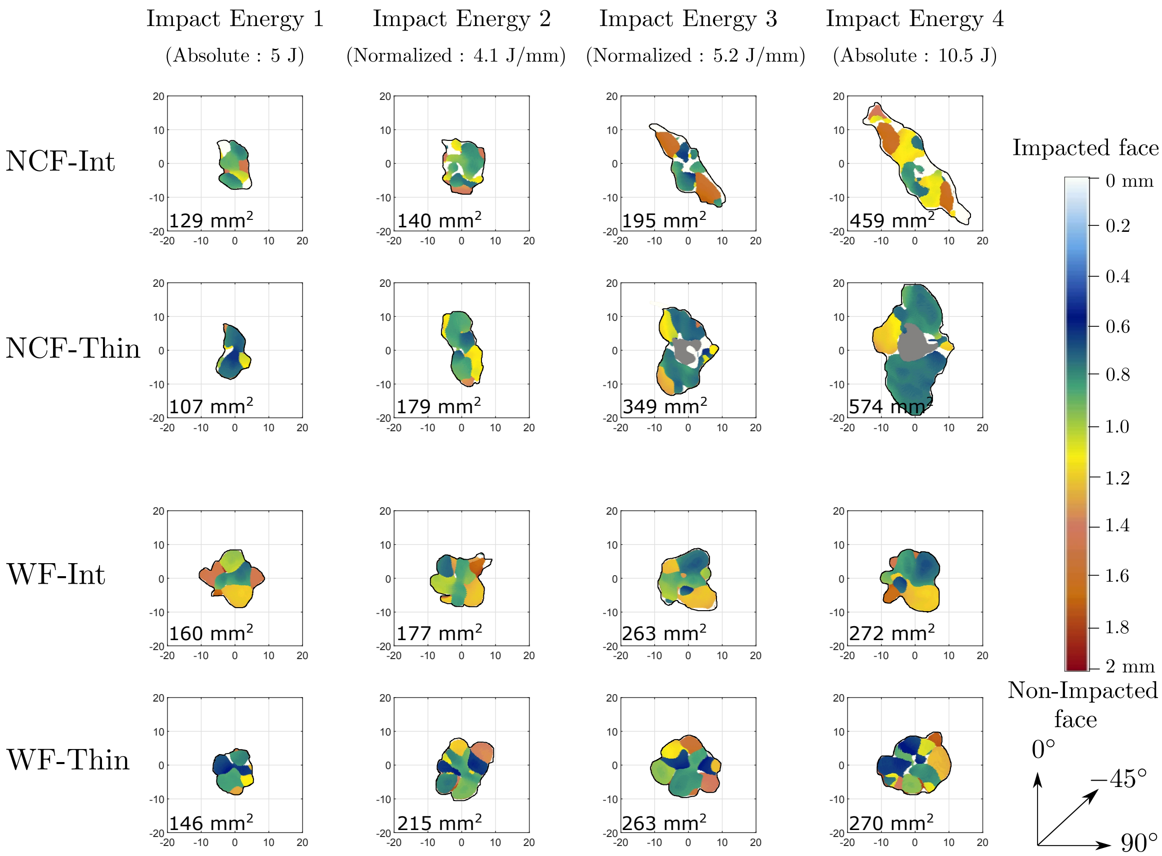

Figure 7: Projected damage contours and areas obtained from the C-scan damage assessment of all laminates for all impact energies (The average projected damage area is presented with the through-the-thickness colour bar. The field of inspection presented is 40 x 40 mm^2).

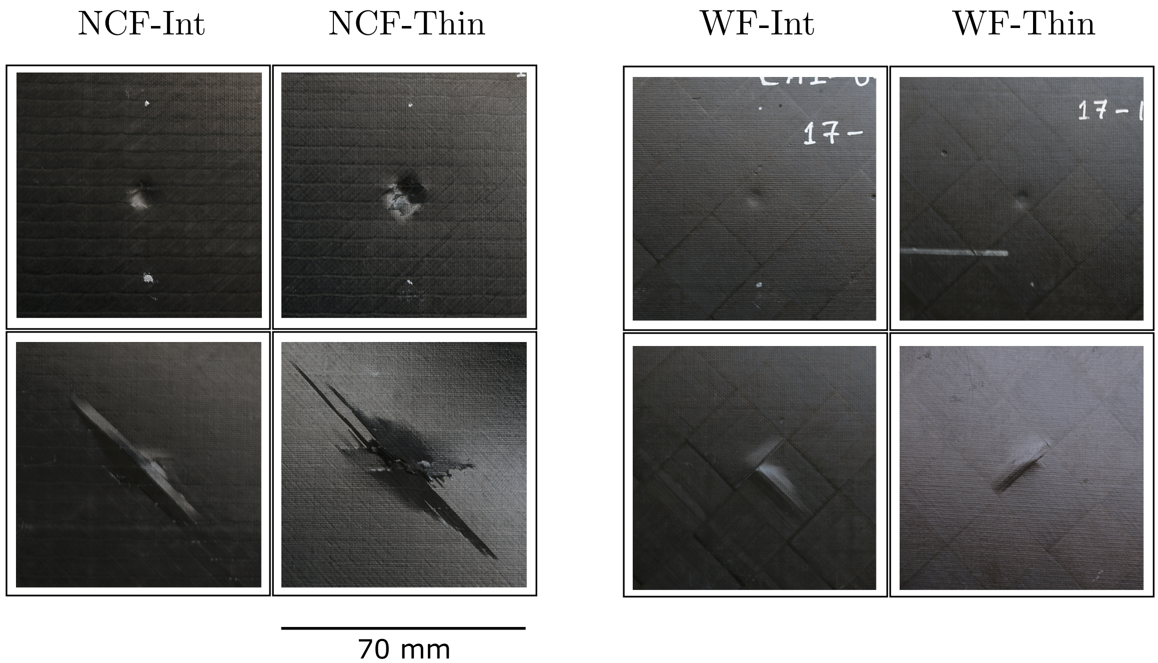

Figure 8: Photos of the impacted (top) and non-impacted (bottom) faces of NCF and WF laminates from the 10.5 J impact test (Each image represents a square window of 70 x 70 mm referenced from the impact centre).

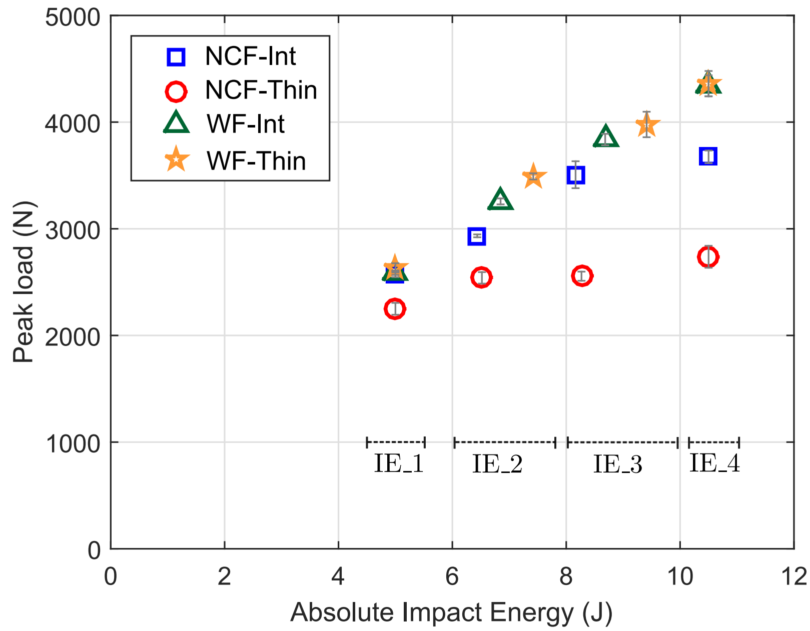

(a)

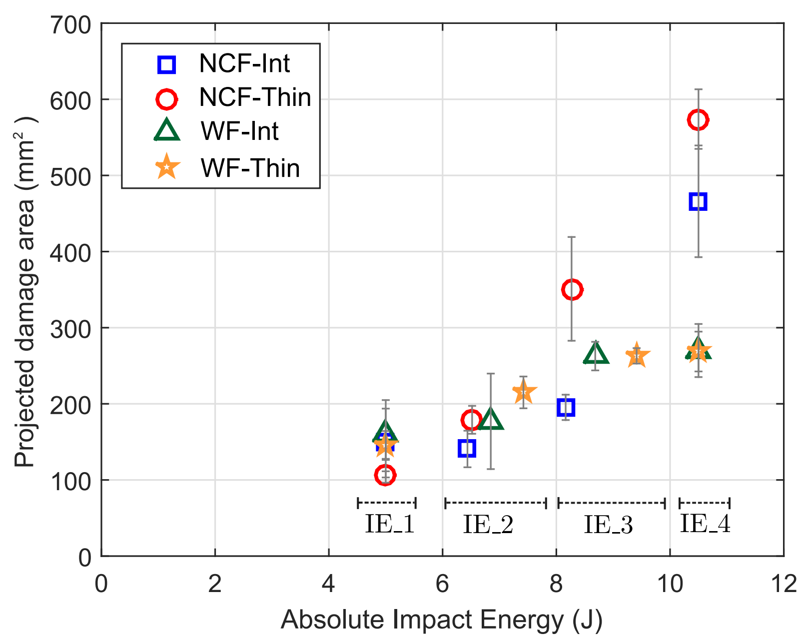

(b)

Figure 9: Impact damage resistance parameters (a) peak load and (b) projected damage area compared between all the laminates for all absolute impact energies (Average value presented along with the standard deviation indicated by the vertical markers).

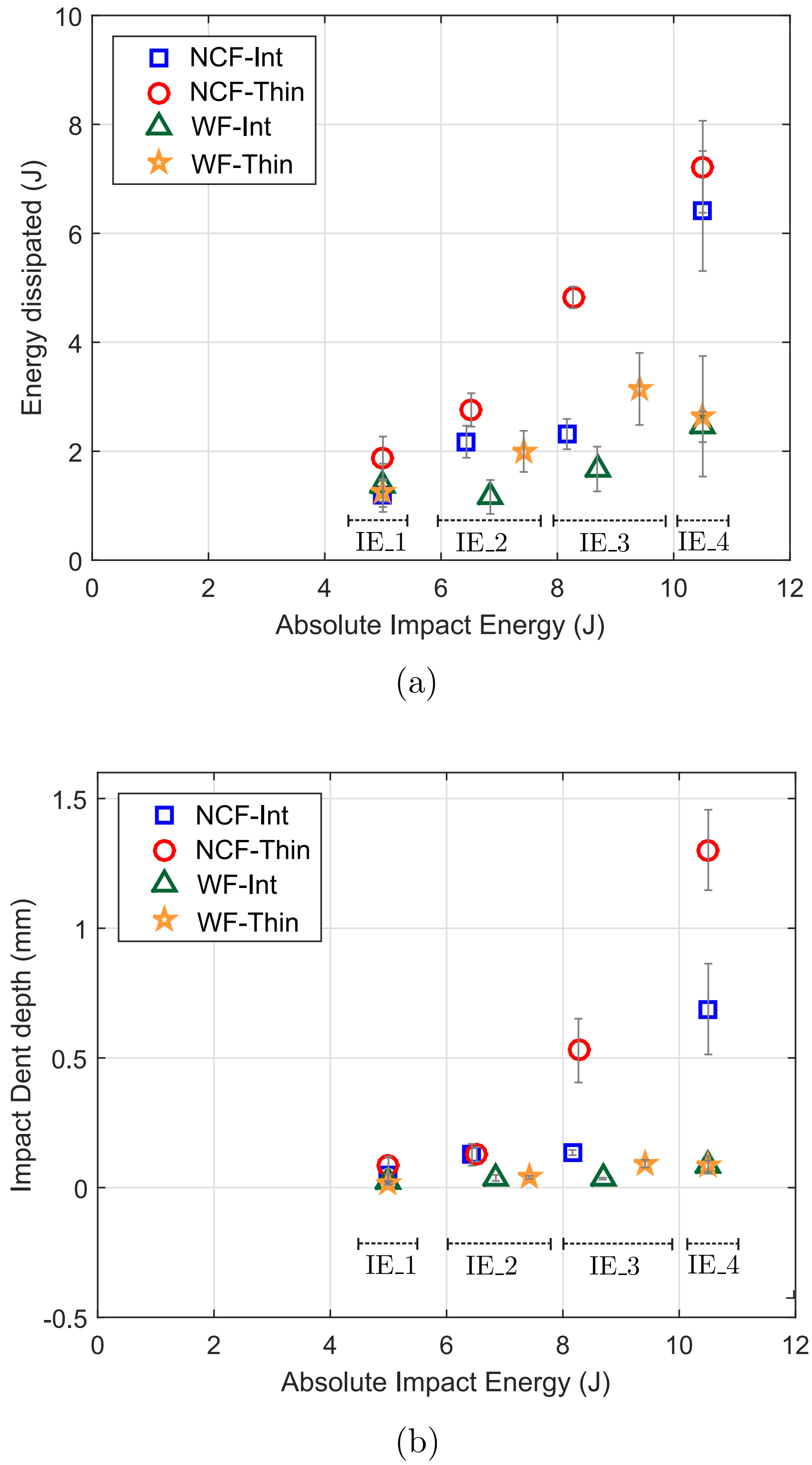

Figure 10: Impact damage resistance parameters (a) dissipated energy and (b) impact dent depth compared between all the laminates for all absolute impact energies (Average value presented along with the standard deviation indicated by the vertical markers).

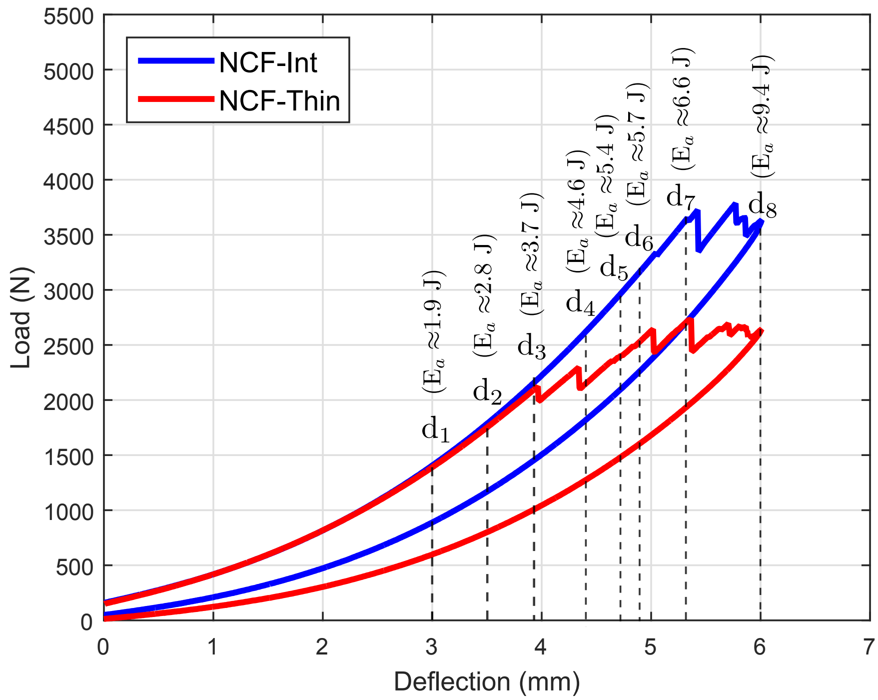

Figure 11: Load-indenter displacement QSI curve for NCF-Int and NCF-Thin for d=6 mm (the other displacement levels used in the study are also marked).

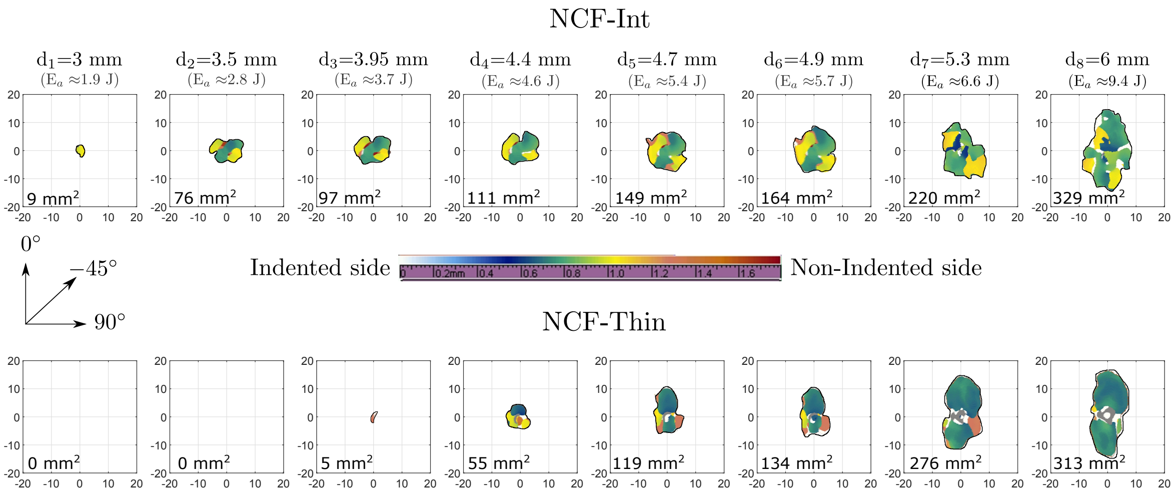

Figure 12: C-scan images comparing the evolution of damage in the NCF laminates for all the indenter displacement levels.

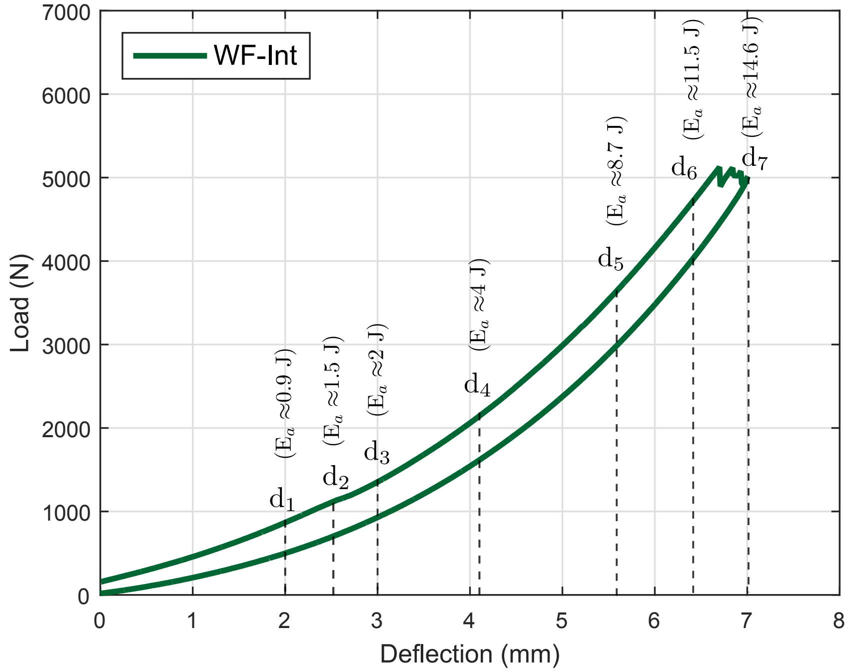

(a)

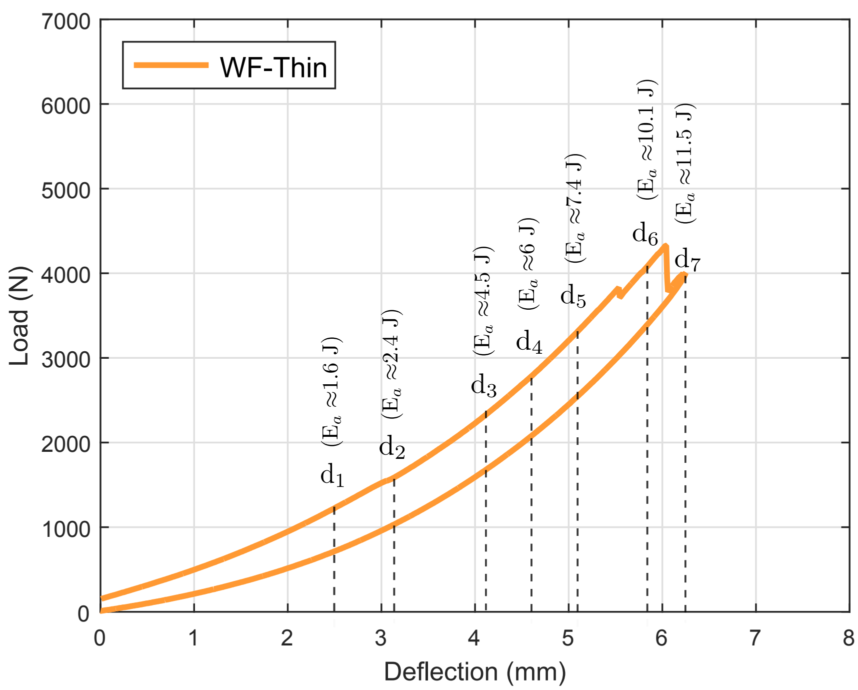

(b)

Figure 13: Load-indenter displacement QSI curve for WF-Int and WF-Thin for d=7 mm and d=6.25 mm, respectively (the other displacement levels used in the study are also marked).

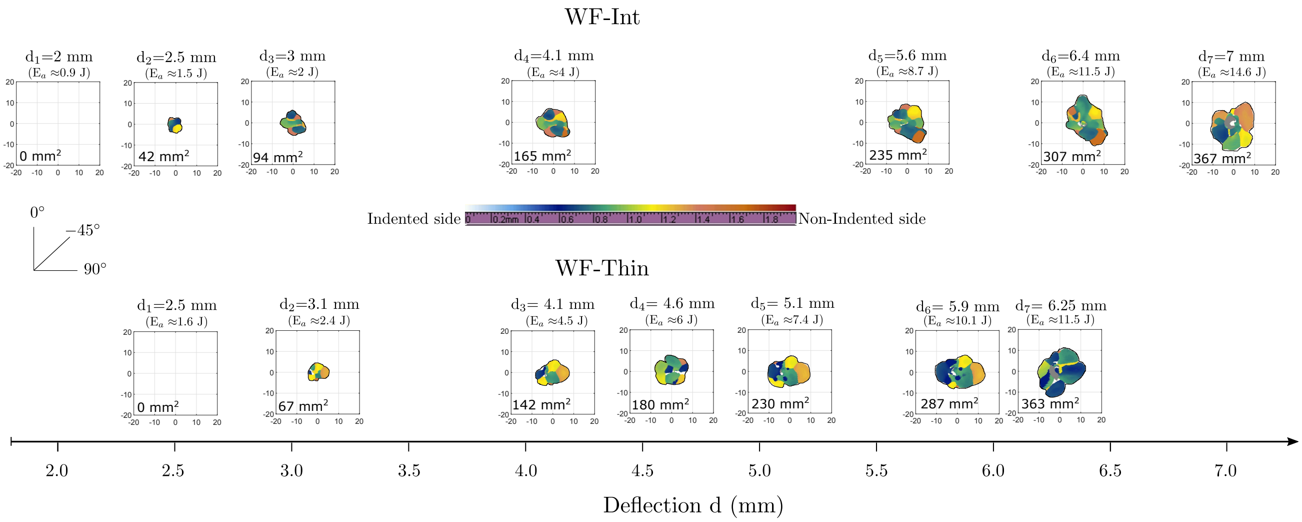

Figure 14: C-scan images showing the damage evolution in WF-Int (top) and WF-Thin (bottom) for all indenter displacement levels. Note that the scans are presented along an indenter deflection on the horizontal axis.

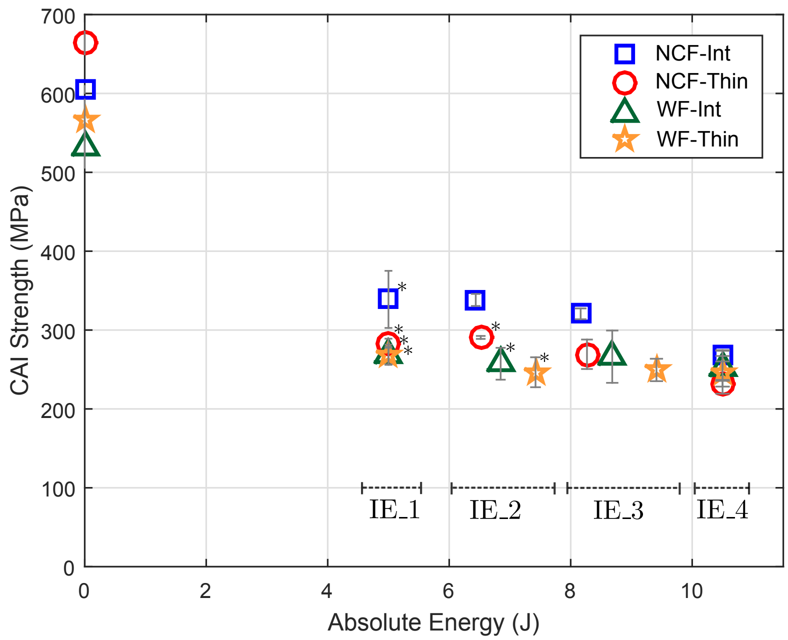

(a)

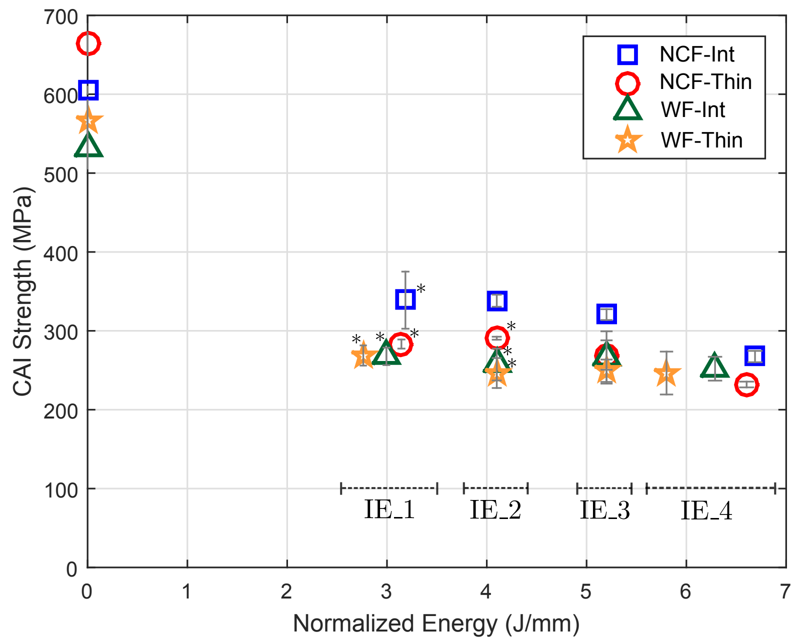

(b)

*CAI failure at the specimen top due to local buckling

Figure 15: Plain compression strength and compression after impact strength values against (a) absolute impact energies and (b) normalized impact energies for all the laminates.

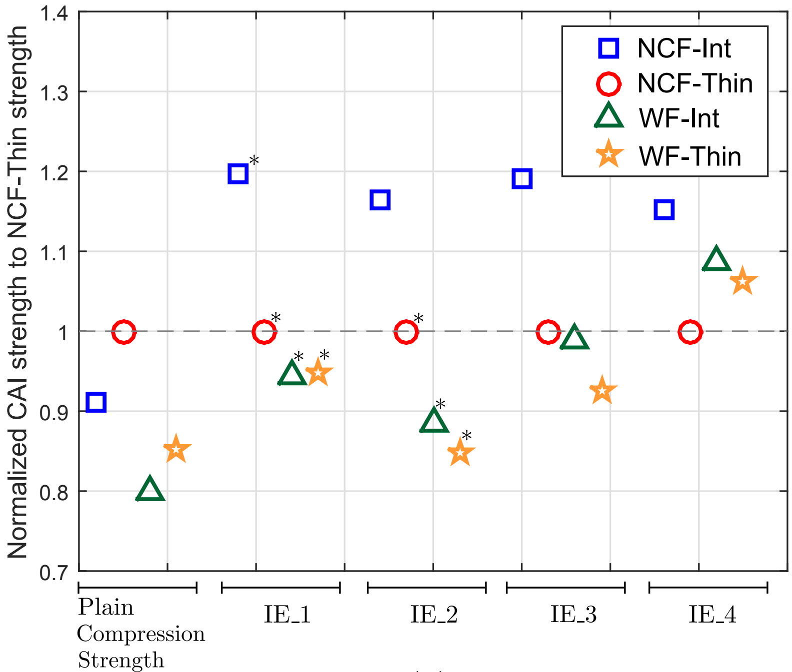

(a)

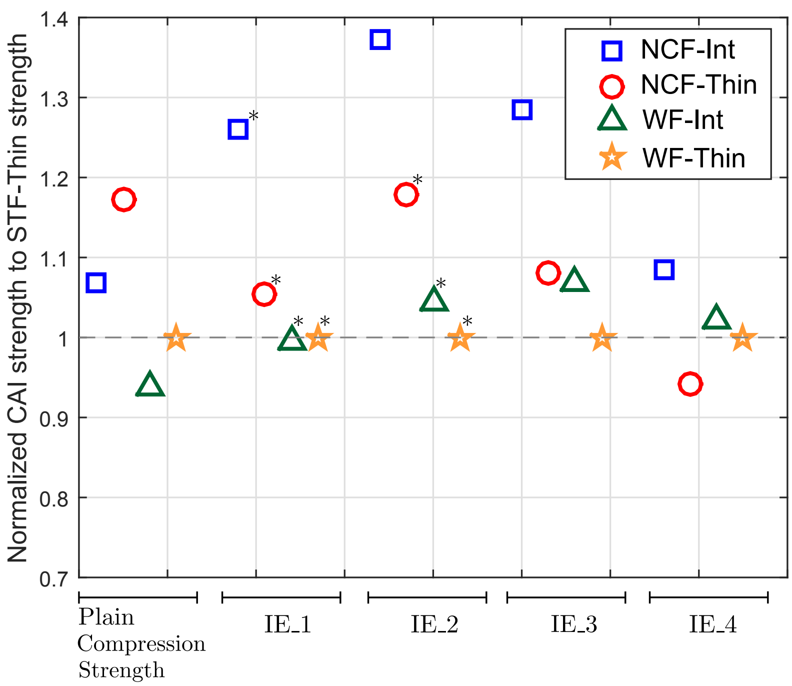

(b)

*CAI failure at the specimen top due to local buckling

Figure 16: Comparison of CAI strength normalized with (a) NCF-Thin as baseline and (b) WF-Thin as baseline. The plain compression strength is also normalized according to the respective baselines.

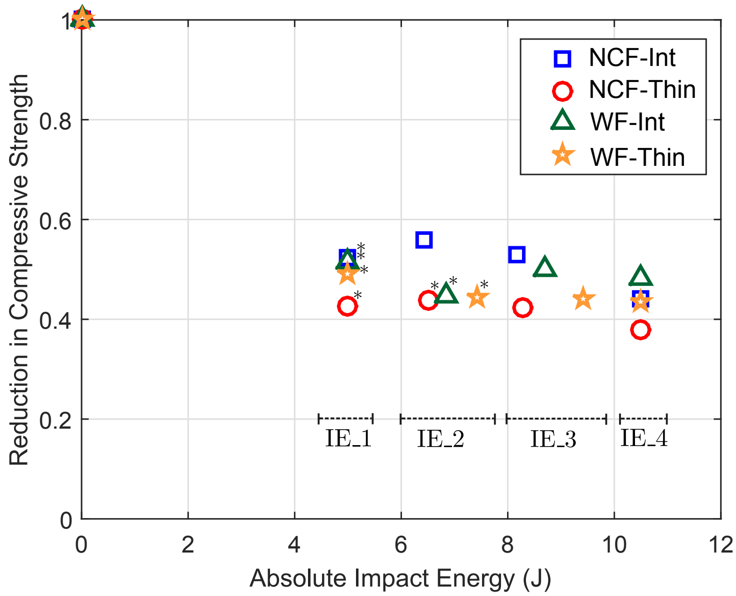

*CAI failure at the specimen top due to local buckling

Figure 17: Normalized reduction in the compressive strength due to the impact damage of all laminates.

Table 1: Laminates and their details

Laminate	Description	Stacking sequence	Fabric grade (g/m^2)	Ply thickness (mm)	Nominal laminate thickness (mm)
NCF-Int	Intermediate plies	$[(45/0)/(-45/90)/(22.5/-22.5)]_S$	268	0.134	1.61
NCF-Thin	Thin plies	$[(45/0)/(-45/90)/(45/0)/(-45/90)/(45/0)/(-45/0)]_S$	134	0.067	1.61
WF-Int	Intermediate plies	$[(45/-45)/(0/90)/(45/-45)/(0/90)]_{\$}$	240	0.12	1.68
WF-Thin	Thin plies	$[((45/-45)/(0/90))_2/(45/-45)/(0/90)]_{\$}$	160	0.08	1.76

Table 2: Laminates and the defined impact energies

Laminate	Measured laminate thickness (mm)	Impact Energy 1: IE_1		Impact Energy 2: IE_2		Impact Energy 3: IE_3		Impact Energy 4: IE_4	
		Abs (J)	Norm (J/mm)	Abs (J)	Norm (J/mm)	Abs (J)	Norm (J/mm)	Abs (J)	Norm (J/mm)
NCF-Int	1.57	5	3.2	6.4	4.1	8.2	5.2	10.5	6.7
NCF-Thin	1.58	5	3.2	6.5	4.1	8.3	5.2	10.5	6.6
WF-Int	1.66	5	3	6.8	4.1	8.7	5.2	10.5	6.3
WF-Thin	1.82	5	2.7	7.5	4.1	9.5	5.2	10.5	5.8